What is more important: the proton heat flux or the electron heat flux ?

Peter Hunana

M. L. Goldstein, T. Passot, P. L. Sulem, D. Laveder, G. P. Zank

Kennebunkport, 2013

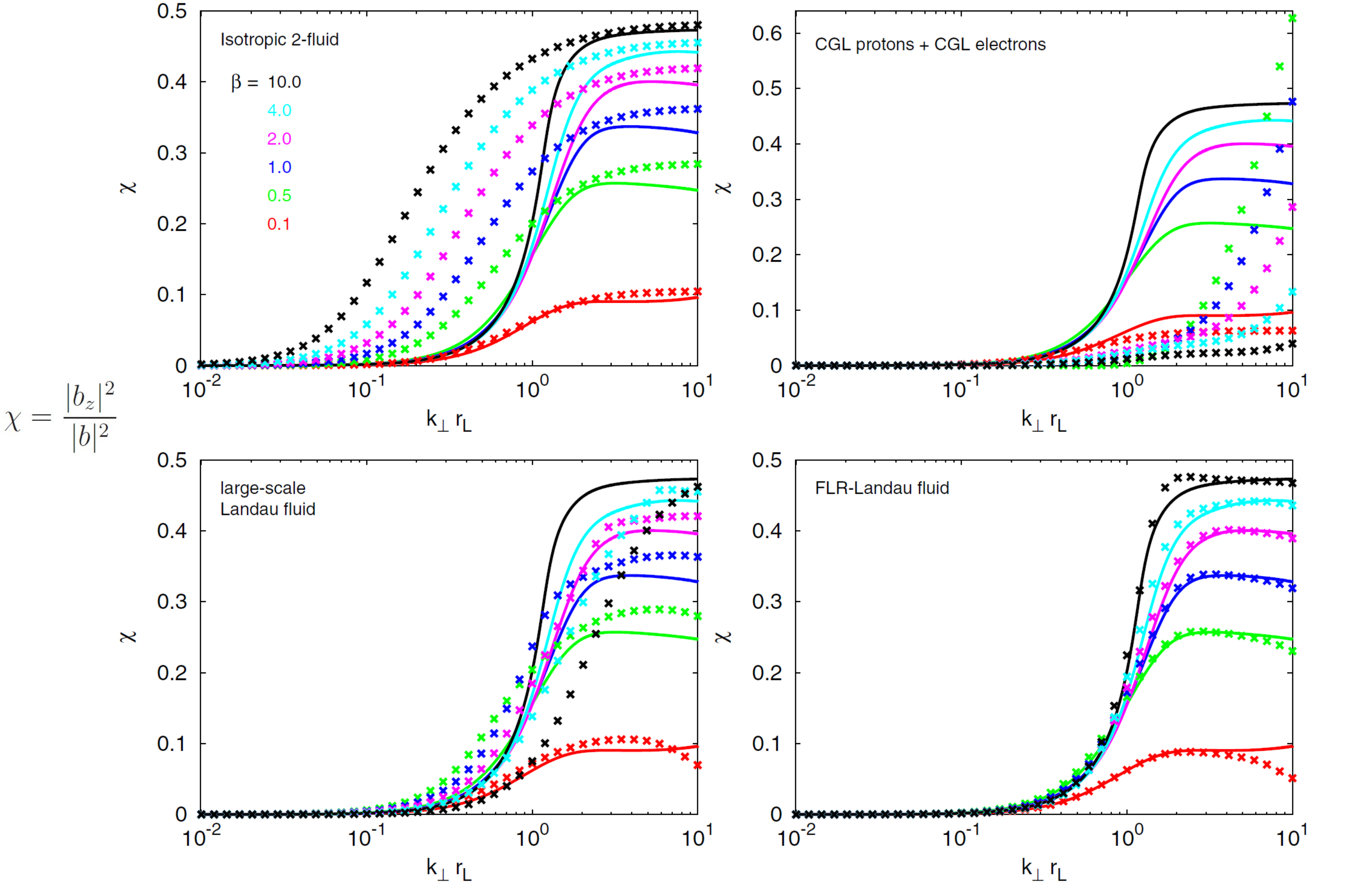

Figure 2. Magnetic compressibility $\chi(k_\perp r_L)$ of highly oblique KAWs with propagation angle $\theta = 89^\circ.99$ for the isotropic two-fluid model (top left), CGL protons + CGL electrons model (top right), large-scale Landau fluid model (bottom left), and FLR-Landau fluid model (bottom right). Solid lines represent kinetic theory and crosses represent solutions of the corresponding fluid models. The proton plasma beta is 0.1 (red), 0.5 (green), 1.0 (blue), 2.0 (magenta), 4.0 (cyan), and 10.0 (black).

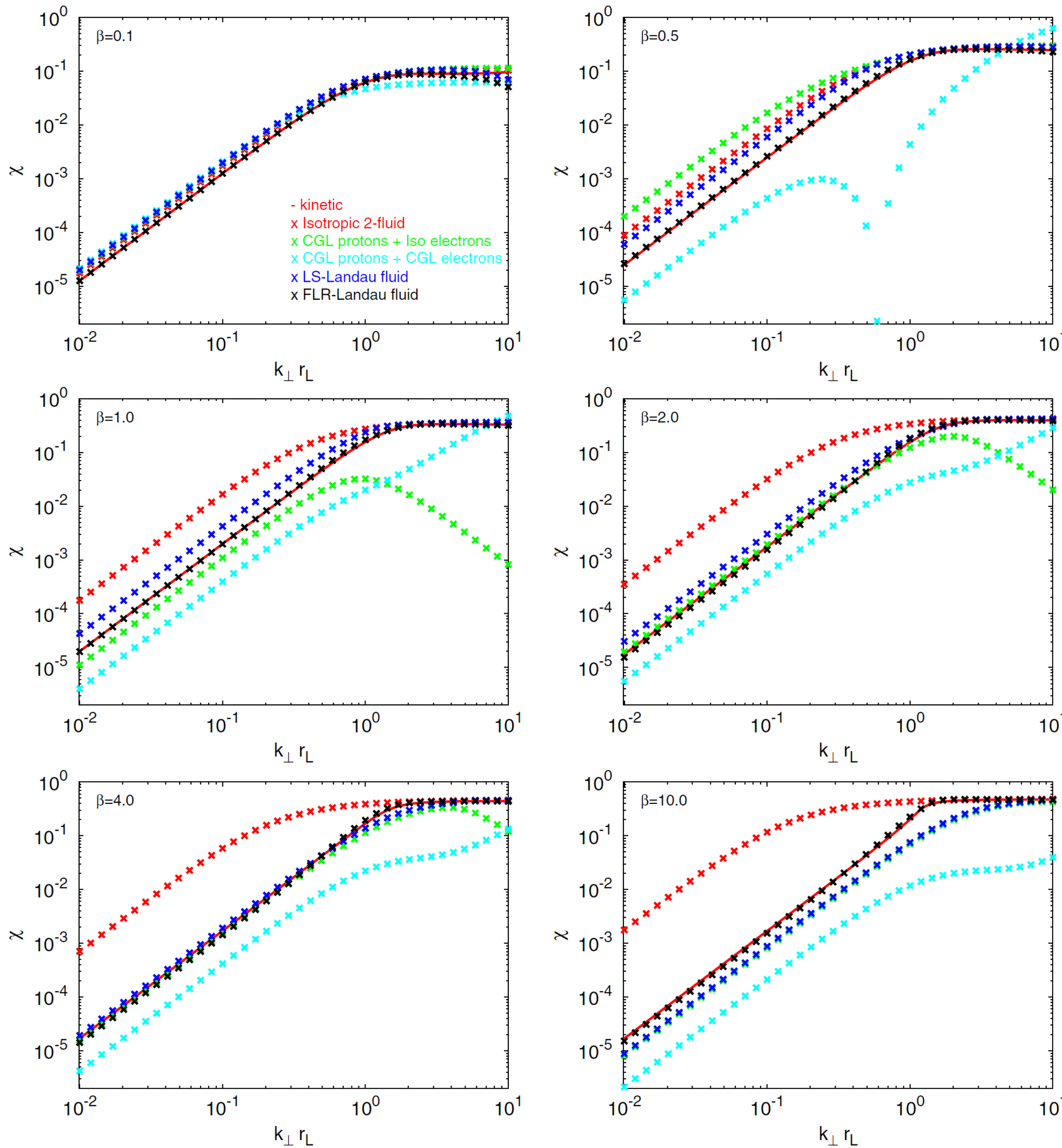

Figure 3. Similar to Figure 2 but with a logarithmic scale for compressibility χ, which emphasizes the large scales. The models are directly compared side by side, separately for each plasma β. The models are kinetic theory (red line), isotropic two-fluid (red crosses), CGL protons + Iso electrons (green crosses), CGL protons + CGL electrons (cyan crosses), LS-Landau fluid (blue crosses), and FLR-Landau fluid (black crosses). The proton plasma beta is 0.1 (top left), 0.5 (top right), 1.0 (center left), 2.0 (center right), 4.0 (bottom left), and 10.0 (bottom right).

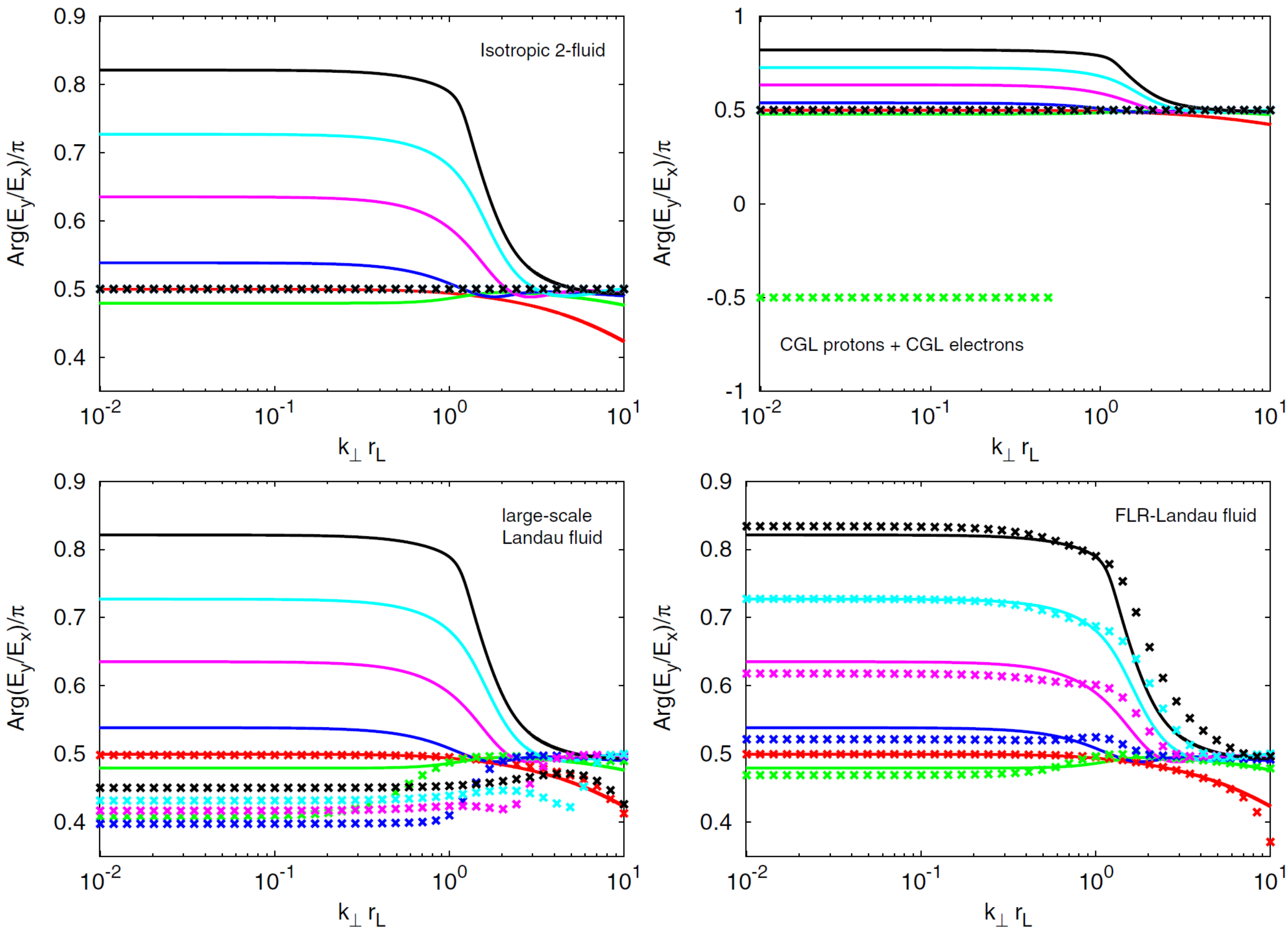

Figure 4. Polarization $\mathcal{P}$ of highly oblique KAWs. As in Figure 2, solid lines represent kinetic theory and the proton plasma beta is 0.1 (red), 0.5 (green), 1.0 (blue), 2.0 (magenta), 4.0 (cyan), and 10.0 (black).

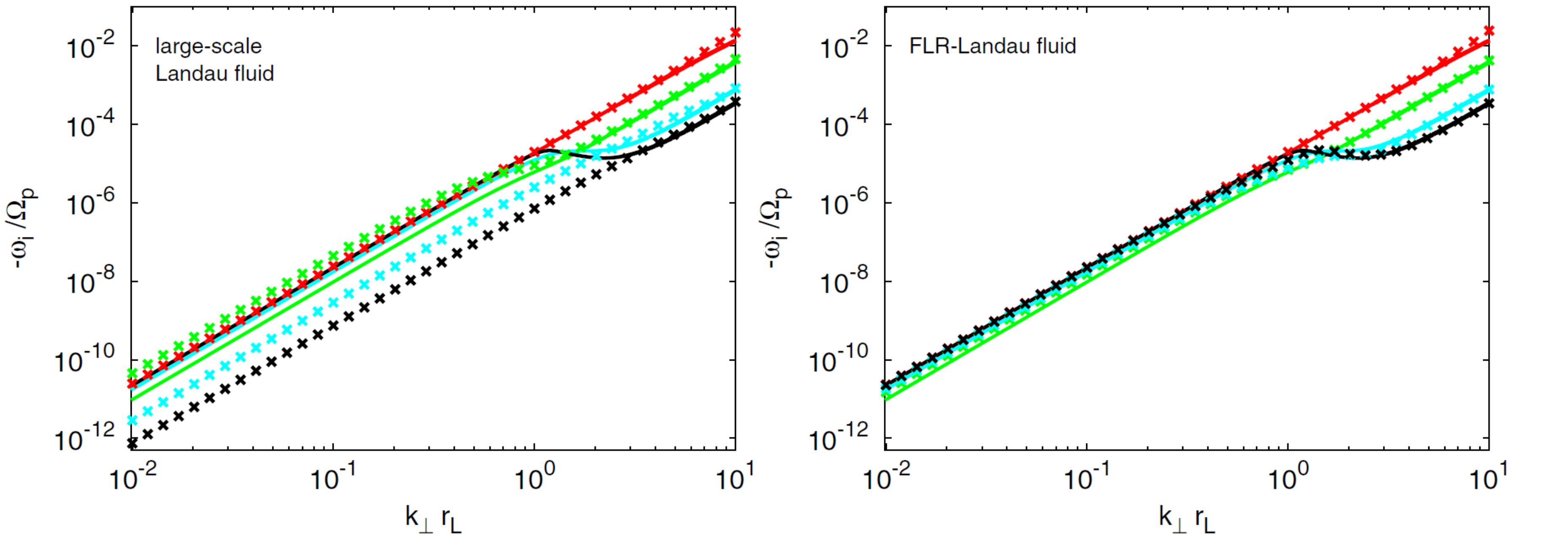

Figure 8. Damping rates of highly oblique KAWs ($\theta = 89\overset{\circ}{.}99$) for large-scale Landau fluid (left) and FLR-Landau fluid (right). Kinetic solutions are solid line fluid solutions are crosses. Proton β is 0.1 (red), 0.5 (green), 4.0 (cyan), and 10.0 (black).

(A color version of this figure is available in the online journal.)

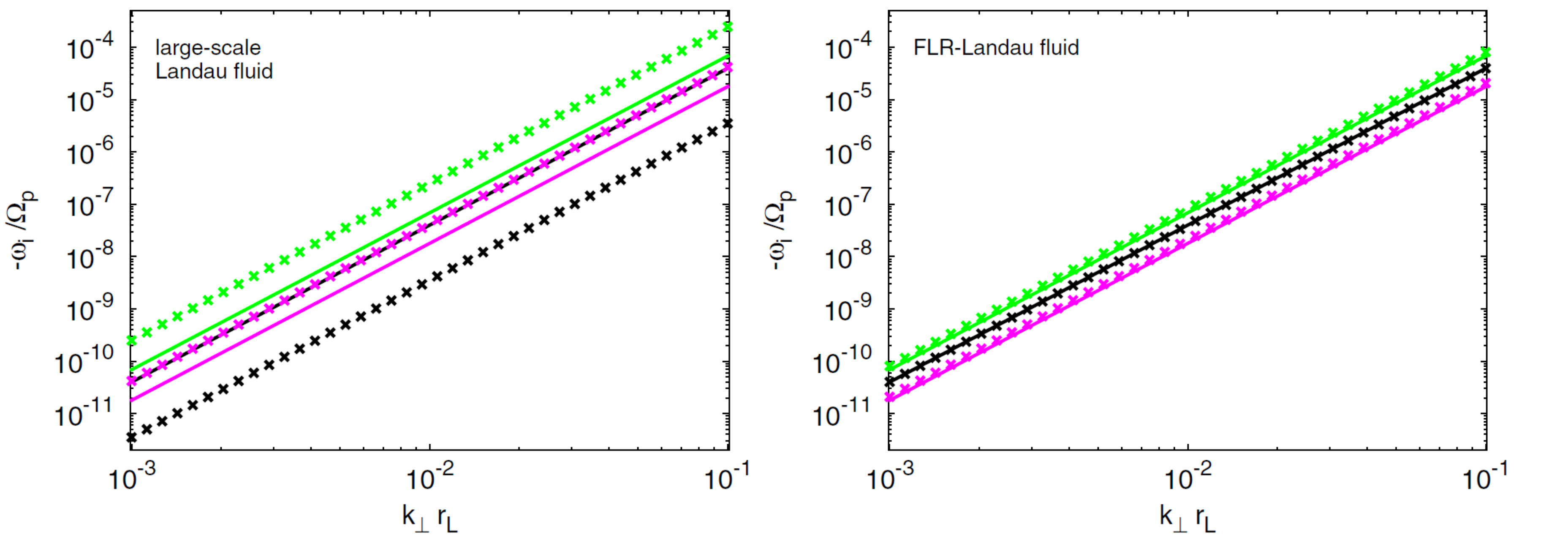

Figure 9. Similar to Figure 8 but at $\theta = 60°$. Proton β is 0.5 (green), 2.0 (magenta), and 10.0 (black).

- Advantage of Landau fluids vs kinetic description:
  you can turn things on/off to see what is important

- Let's put the electron heat flux to zero and use
  the FLR-Landau fluid model with isothermal electrons

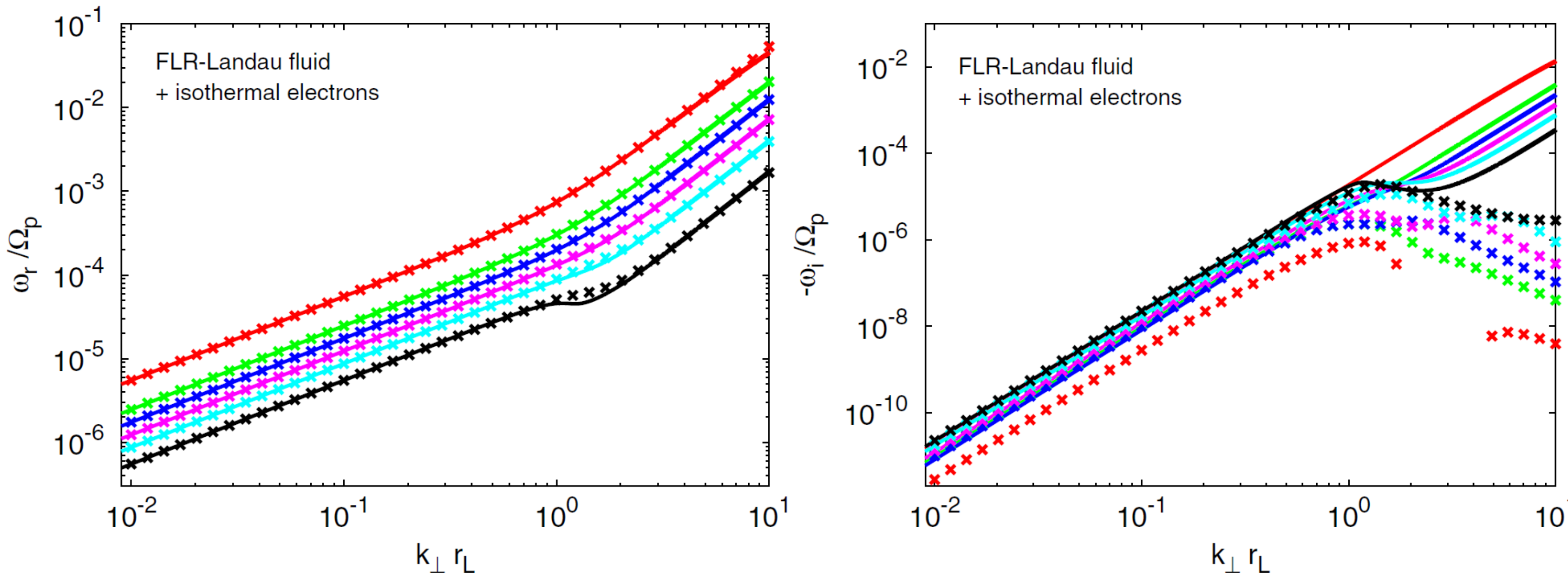

Figure 10. Real frequency ω_r/Ω_p (left) and imaginary frequency $-\omega_i/\Omega_p$ (right) for highly oblique KAWs ($\theta = 89.^\circ99$) calculated from FLR-Landau fluid model with isothermal electrons. The figure demonstrates the importance of electron Landau damping for ω_i even at scales comparable to the proton gyroscale $k_\perp r_L \sim 1$. Colors for proton β are the same as in Figure 2.

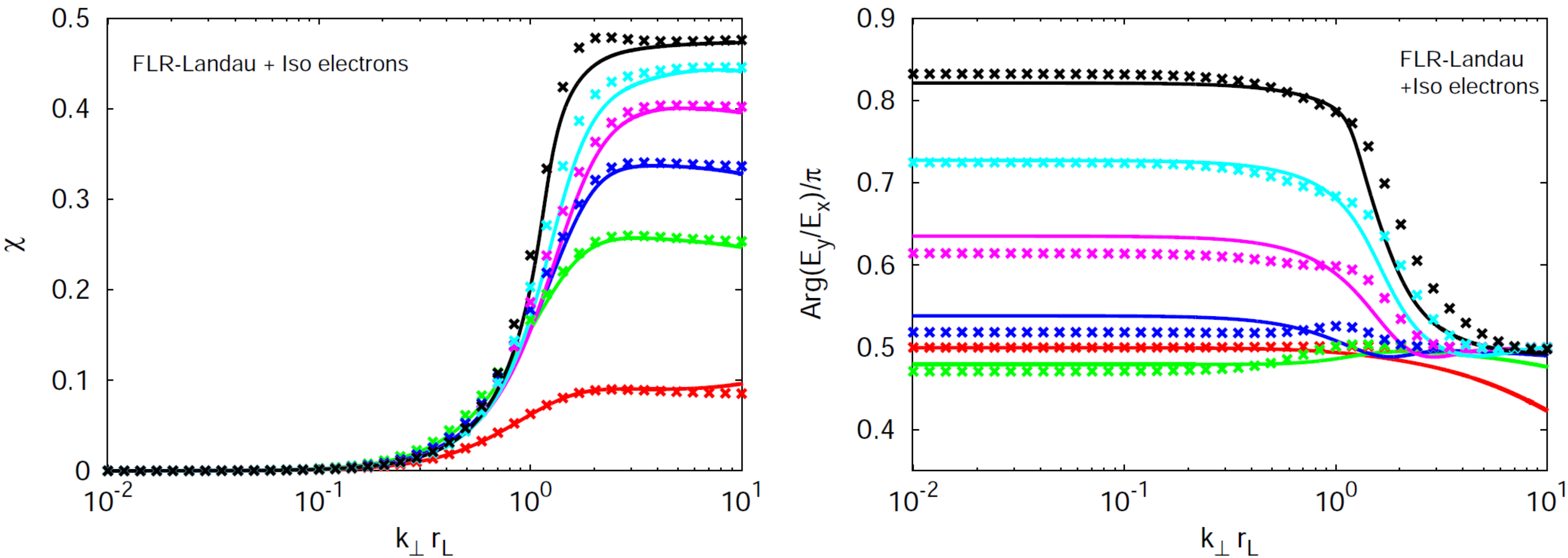
FLR-Landau + Iso electrons
χ
$k_\perp r_L$
FLR-Landau
+Iso electrons
$Arg(E_y/E_x)/\pi$
$k_\perp r_L$

- Now you will say that there is a direct observational evidence that the electron heat flux is the largest...

- I am not saying that it is not

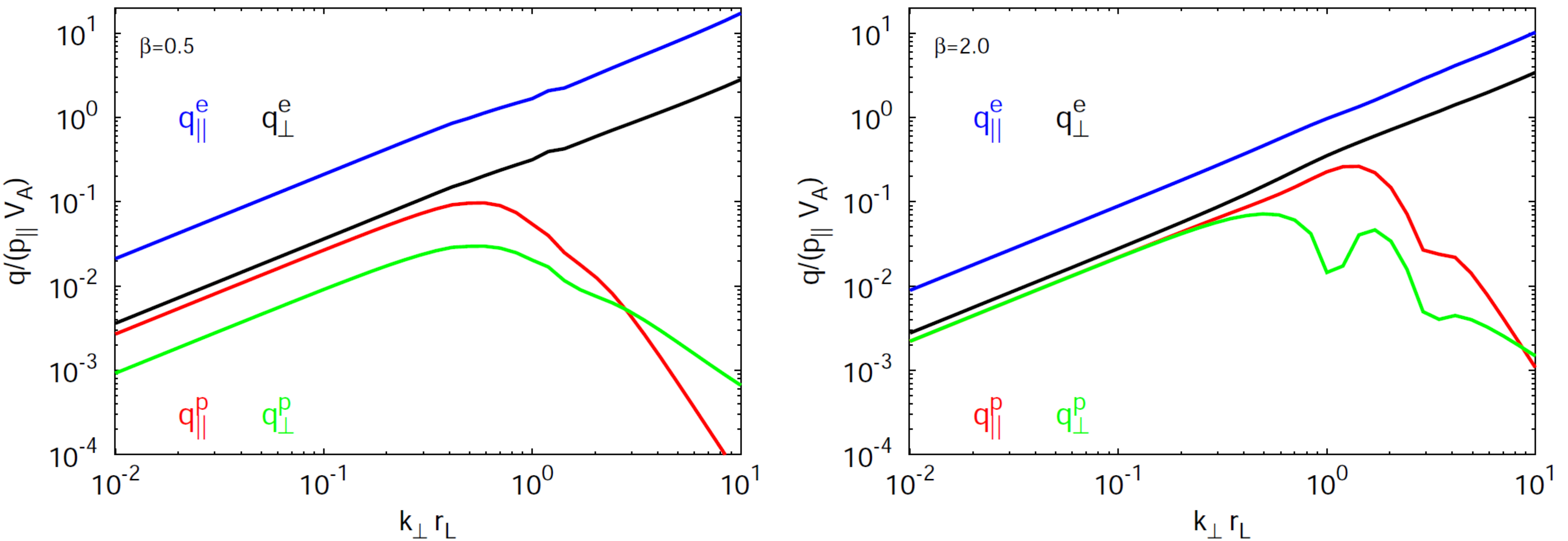

β=0.5
$q^e_{||}$
$q^e_\perp$
$q^p_{||}$
$q^p_\perp$
q/(p|| VA)
k⊥ rL
β=2.0
$q^e_{||}$
$q^e_\perp$
$q^p_{||}$
$q^p_\perp$
q/(p|| VA)
k⊥ rL

- Is it correct to say that the electron heat flux is the largest in the solar wind ? Yes it is.
- However, is it correct to say that the electron heat flux is the most important one ? No it isn't. This statement is scale dependent. At scales comparable or larger than the proton gyroscale, the proton heat is the most important one.
- Coupling of a MHD code at large scales with a kinetic code at small scales might never work.
- What might work are hybrid simulations where protons are modeled kinetically and electrons are modeled by a Landau fluid description.

Large-scale Landau fluid

$$p_{\|r} = \mathbf{p}_r : \hat{\boldsymbol{b}}\hat{\boldsymbol{b}}$$

$$p_{\perp r} = \mathbf{p}_r : (\mathbf{I} - \hat{\boldsymbol{b}}\hat{\boldsymbol{b}})/\mathbf{2}$$

$$\partial_t p_{\perp r} + \nabla \cdot (\boldsymbol{u}_r p_{\perp r}) + p_{\perp r} \nabla \cdot \boldsymbol{u}_r - p_{\perp r} \hat{\boldsymbol{b}} \cdot \nabla \boldsymbol{u}_r \cdot \hat{\boldsymbol{b}} \\ + \nabla \cdot (q_{\perp r} \hat{\boldsymbol{b}}) + q_{\perp r} \nabla \cdot \hat{\boldsymbol{b}} = 0, \qquad \text{(A10)}$$

$$\partial_t p_{\|r} + \nabla \cdot (\boldsymbol{u}_r p_{\|r}) + 2 p_{\|r} \hat{\boldsymbol{b}} \cdot \nabla \boldsymbol{u}_r \cdot \hat{\boldsymbol{b}} \\ + \nabla \cdot (q_{\|r} \hat{\boldsymbol{b}}) - 2 q_{\perp r} \nabla \cdot \hat{\boldsymbol{b}} = 0. \qquad \text{(A11)}$$

$$\mathbf{S}_r^{\|} = \mathbf{q}_r : \hat{\boldsymbol{b}}\hat{\boldsymbol{b}}$$

$$\mathbf{S}_r^{\perp} = \mathbf{q}_r : (\mathbf{I} - \hat{\boldsymbol{b}}\hat{\boldsymbol{b}})/\mathbf{2}$$

$$q_{\|r} = \mathbf{S}_r^{\|} \cdot \hat{\boldsymbol{b}}$$

$$q_{\perp r} = \mathbf{S}_r^{\perp} \cdot \hat{\boldsymbol{b}}$$

$$\partial_t q_{\|r} + \nabla \cdot (q_{\|r} \boldsymbol{u}_r) + 3 q_{\|r} \hat{\boldsymbol{b}} \cdot \nabla \boldsymbol{u}_r \cdot \hat{\boldsymbol{b}} + 3 p_{\|r} (\hat{\boldsymbol{b}} \cdot \nabla) \left(\frac{p_{\|r}}{\rho_r} \right) \\ + \nabla \cdot (\tilde{r}_{\|\|r} \hat{\boldsymbol{b}}) - 3 \tilde{r}_{\|\perp r} \nabla \cdot \hat{\boldsymbol{b}} = 0 \qquad \text{(A12)}$$

$$\partial_t q_{\perp r} + \nabla \cdot (q_{\perp r} \boldsymbol{u}_r) + q_{\perp r} \nabla \cdot \boldsymbol{u}_r + p_{\|r} (\hat{\boldsymbol{b}} \cdot \nabla) \left(\frac{p_{\perp r}}{\rho_r} \right) \\ + \nabla \cdot (\tilde{r}_{\|\perp r} \hat{\boldsymbol{b}}) + \left((p_{\|r} - p_{\perp r}) \frac{p_{\perp r}}{\rho_r} - \tilde{r}_{\perp\perp r} + \tilde{r}_{\|\perp r} \right) \\ \times (\nabla \cdot \hat{\boldsymbol{b}}) = 0. \qquad \text{(A13)}$$

$$\tilde{r}_{\|\|r} = \frac{32 - 9\pi}{2(3\pi - 8)} n_0 v_{\mathrm{th}\|r}^2 T'_{\|r} - \frac{2\sqrt{\pi}}{3\pi - 8} v_{\mathrm{th}\|r} \frac{ik_z}{|k_z|} q_{\|r}, \tag{A14}$$

$$\tilde{r}_{\|\perp p} = -\frac{\sqrt{\pi}}{2} v_{\mathrm{th}\|p} \frac{ik_z}{|k_z|} \times \left[q_{\perp p} + \frac{1}{\Omega_p} \frac{\overline{p}_{\perp p}}{\rho_0} (\overline{p}_{\perp p} - \overline{p}_{\| p}) \left(i\boldsymbol{k}_\perp \times \frac{\boldsymbol{B}_\perp}{B_0} \right)_z \right], \tag{A15}$$

$$\tilde{r}_{\|\perp e} = -\frac{\sqrt{\pi}}{2} v_{\mathrm{th}\|e} \frac{ik_z}{|k_z|} \times \left[q_{\perp e} - \frac{1}{\Omega_p} \frac{\overline{p}_{\perp e}}{\rho_0} (\overline{p}_{\perp e} - \overline{p}_{\| e}) \left(i\boldsymbol{k}_\perp \times \frac{\boldsymbol{B}_\perp}{B_0} \right)_z \right], \tag{A16}$$

$$\tilde{r}_{\perp\perp r} = 0. \tag{A17}$$

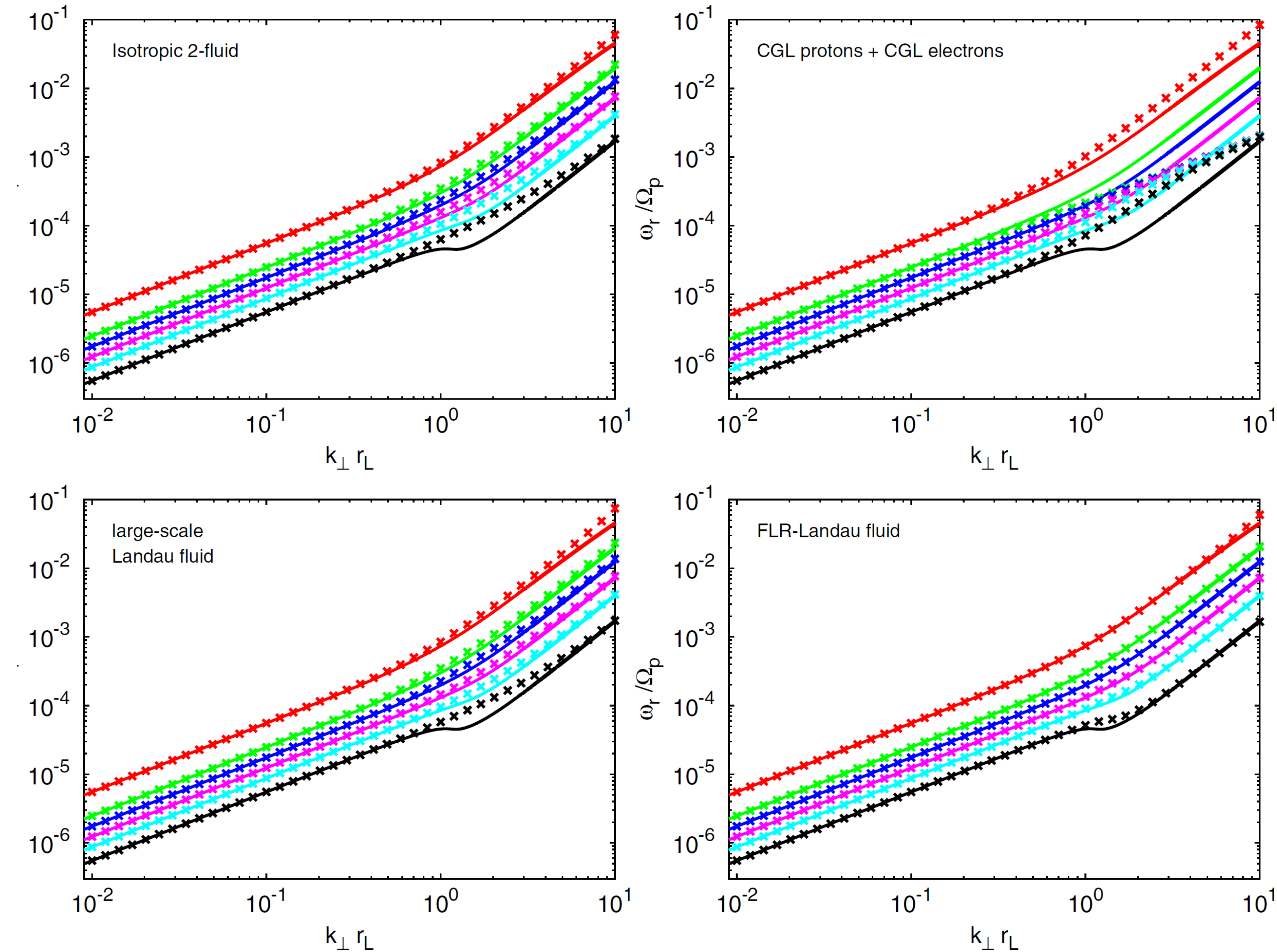

Figure 5. Real frequency of highly oblique KAWs; all parameters are the same as in Figure 2.

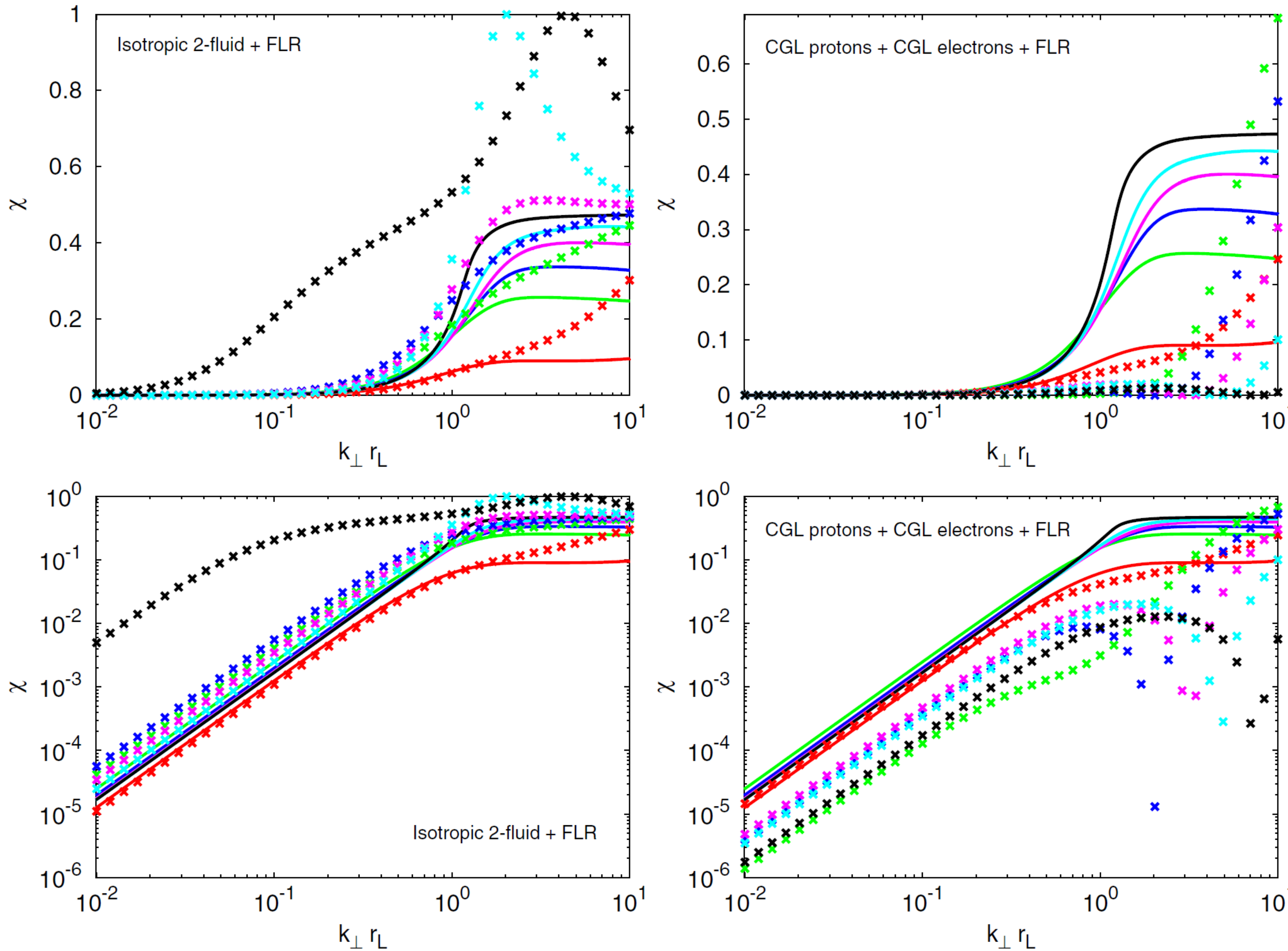

Figure 11. Compressibility χ of KAWs with $\theta = 89^\circ.99$ for the isotropic two-fluid + FLR model (left column) and the CGL proton + CGL electrons + FLR model (right column). Top panels have the χ in a linear scale, while bottom panels in a logarithmic scale. Kinetic solutions are solid lines and fluid solutions are crosses. Proton β is 0.1 (red), 0.5 (green), 1.0 (blue), 2.0 (magenta), 4.0 (cyan), and 10.0 (black).

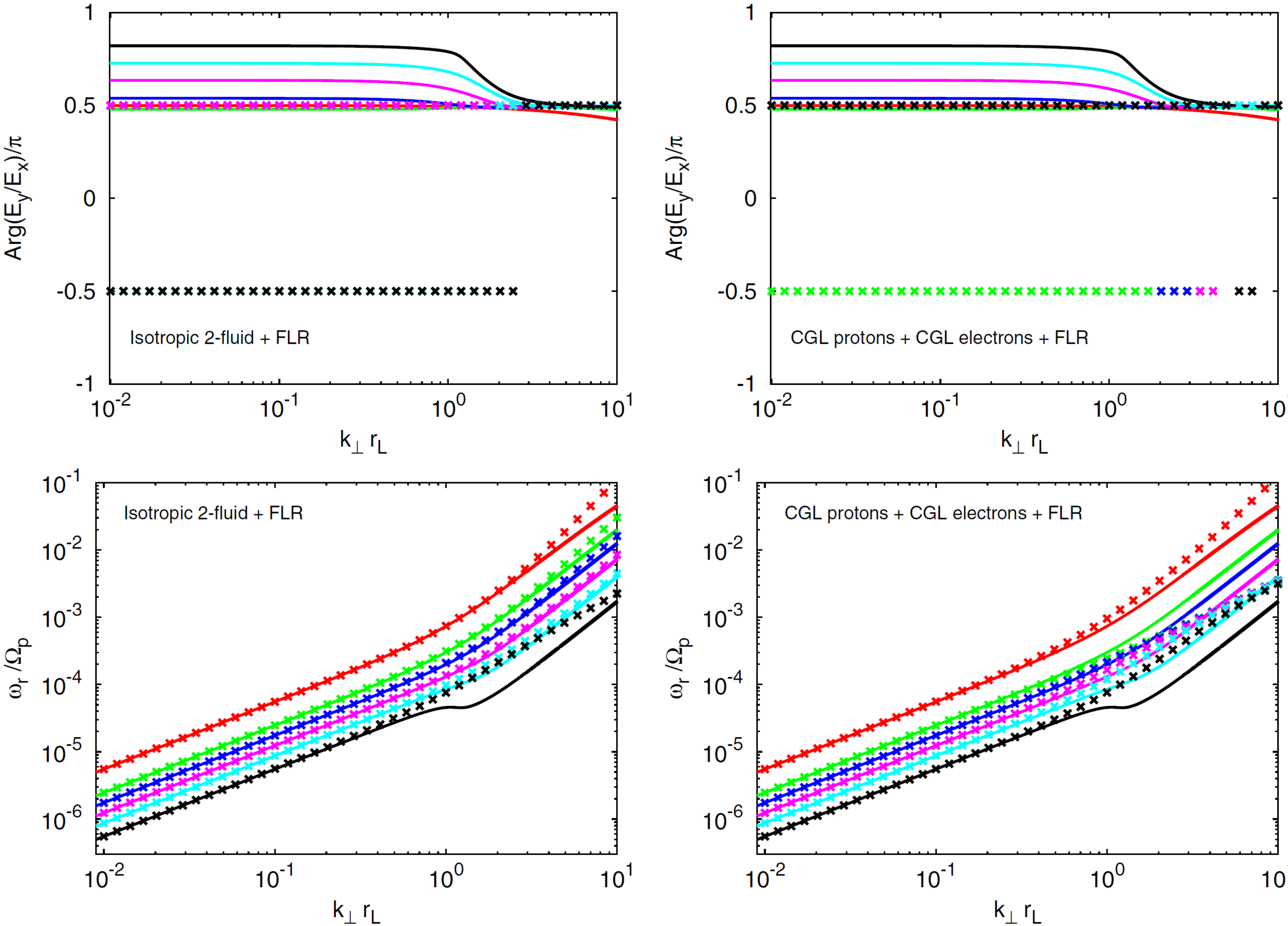

Figure 12. Polarization $\mathcal{P}$ (top) and real frequency ω_r/Ω_p (bottom), all parameters are the same as in Figure 11.

FLR-Landau fluid model

$$\partial_t p_{\perp r} + \nabla \cdot (\vec{u}_r p_{\perp r}) + p_{\perp r} \nabla \cdot \vec{u}_r - p_{\perp r} \hat{b} \cdot \nabla \vec{u}_r \cdot \hat{b}$$
$$+ \frac{1}{2} \left(\mathrm{tr}\, \nabla \cdot \mathbf{q}_r - \hat{b} \cdot (\nabla \cdot \mathbf{q}_r) \cdot \hat{b} \right)$$
$$+ \frac{1}{2} \left(\mathrm{tr}\, (\Pi \cdot \nabla \vec{u}_r)^S - (\Pi \cdot \nabla \vec{u}_r)^S : \boldsymbol{\tau} + \Pi : \frac{d\boldsymbol{\tau}}{dt} \right)_r \delta_{rp} = 0, \tag{5}$$

$$\partial_t p_{||r} + \nabla \cdot (\vec{u}_r p_{||r}) + 2p_{||r} \hat{b} \cdot \nabla \vec{u}_r \cdot \hat{b} + \hat{b} \cdot (\nabla \cdot \mathbf{q}_r) \cdot \hat{b}$$
$$+ \left((\Pi \cdot \nabla \vec{u}_r)^S : \boldsymbol{\tau} - \Pi : \frac{d\boldsymbol{\tau}}{dt} \right)_r \delta_{rp} = 0, \tag{6}$$

FLR stress forces, fully nonlinear (disappear at the linear level),
can produce strong heating both in parallel and perpendicular direction